Journal of Applied Phycology
https://doi.org/10.1007/s10811-025-03681-z

RESEARCH

Valorization of the cell wall polysaccharides of commercially cultivated *Ulva ohnoi* in Mexico

Yolanda Freile-Pelegrín[1] · Daniel Robledo[1] · Cresencia Chávez-Quintal[1] · Juan Bautista Chalé-Dzul[2] · José A. Zertuche-González[3]

Received: 21 July 2025 / Revised: 8 September 2025 / Accepted: 13 September 2025
© The Author(s) 2025

Abstract

Ulva represents an important raw material due to its nutritional value. In addition, it contains cell wall polysaccharides, attractive for various applications. *Ulva ohnoi* is commercially cultivated in Baja California (México) and successfully marketed as human food. The valorization of this biomass as a source of ulvans and cellulose is proposed through a sequential extraction approach. As a first step, an ulvan with a 22.7% yield dry weight, high sulfate and uronic acids content, and with antioxidant capacity was obtained directly from the biomass. From the residual biomass, a semi-crystalline cellulose was recovered (3.8%) with potential for use in encapsulation and biocomposites. Fourier transform infrared (FTIR), and X-ray diffraction (XRD) analysis confirmed the structure of ulvans and cellulose and characterized the crystalline structure of the polysaccharides. Furthermore, using environmentally friendly technology through microwave-assisted extraction (MAE) and ionic liquid (IL), a cellulose derivative (CD) was isolated in the form of microcellulose, as observed by scanning electron microscopy. The results reinforced the potential of this species to diversify its use.

Keywords *Ulva ohnoi* · Chlorophyta · Polysaccharides · Ulvans · Cellulose

Introduction

Seaweed farming has increased in recent decades due to the demand for raw materials for human consumption. One of the commercially important genera is the chlorophyte *Ulva*. This genus can grow in a wide range of salinities and temperatures, showing a high cultivation potential (Zertuche-González et al. 2021) and represents a promising raw material for food due to its content of proteins, pigments, vitamins and polyunsaturated fatty acids (Harsha Mohan et al. 2023). In addition, *Ulva* contains important cell wall polysaccharides such as ulvan and cellulose. Ulvan is a soluble polysaccharide that contains uronic acids (glucuronic and iduronic acids), rhamnose, xylose, and sulfate groups. In this complex sulfated polysaccharide, the rhamnose content, a rare sugar commonly found in bacteria and plants, and iduronic acid content, which has not been identified in other polysaccharides of algal origin, is of great economical interest since it possesses attractive physicochemical properties and biological activities (García-Márquez et al. 2023). Moreover, ulvan, as a biopolymer, has demonstrated diverse potential applications. To date, it has been blended with various structures—including membranes, particles, hydrogels, three-dimensional porous frameworks, and nanofibers—which have been explored for drug delivery and tissue engineering, resulting in a range of innovative applications (Tziveleka et al. 2019).

In addition to ulvan, *Ulva* also stands out for its cellulose content (Siddhanta et al. 2009, 2011; Wahlström et al. 2020). Cellulose is the most abundant renewable carbon source on Earth and constitutes an important structural component of the cell wall in both lower and higher plants. The annual global cellulose production is approximately 180 million

✉ Yolanda Freile-Pelegrín
yolanda.freile@cinvestav.mx

[1] Centro de Investigación y de Estudios Avanzados (Cinvestav), Departamento de Recursos del Mar, Unidad Mérida, Km 6 Carretera Antigua a ProgresoCordemex, 97319 Mérida, Yucatán, México

[2] Hospital de Especialidad, Unidad de Investigación Médica Yucatán, Instituto Mexicano del Seguro Social (IMSS), Calle 41439, Mérida, Yucatán 97150, México

[3] Instituto de Investigaciones Oceanológicas (IIO), México-PROMAC-Blue Evolution, Universidad Autónoma de Baja California (UABC), Ensenada, México

Published online: 14 October 2025

tonnes, primarily for papermaking (Małachowska et al. 2020), as well as for a wide range of applications such as food packaging, food additives, pharmaceutical and biomedical applications, and bioenergy production (Zhao et al. 2022). Thus, the cellulose market industry is projected to grow from US$ 24.11 billion in 2023 to US$ 44.5 billion by 2030 (Nagrale 2023). Chemically, cellulose is a linear polysaccharide consisting of D-glucose subunits linked by β-(1,4)-glycosidic bonds. Each cellulose monomer has three hydroxyl groups per glucose unit capable of forming hydrogen bonds to produce elementary fibrils, which are then packed into larger units called microfibrils, and which in turn form cellulosic fibers containing ordered regions (crystalline) and disordered (amorphous-like). In the ordered regions, cellulose chains are tightly packed together and stabilized by a strong intra- and intermolecular hydrogen-bond (Moon et al. 2011). The relative amount of crystalline material in cellulose, known as the crystallinity index (CI), depends on both its natural source and the extraction procedure. This, in turn, influences its physical, mechanical, chemical, and morphological properties, thereby affecting its overall applicability (Heinze et al. 2018; Trache et al. 2020). During cellulose extraction non-cellulosic constituents such as lignin must be eliminated. Lignin, a highly branched aromatic polymer, is firmly bonded to cellulose, creating a robust structure that is recalcitrant to depolymerization. Due to its structural complexity chemical treatments are used which are energy consuming and generate effluents with serious environmental problems. Although the presence of true lignin in nonvascular organisms has not been confirmed, lignin-like compounds, usually related to polyphenolic compounds, have been identified in seaweeds including green algae (Delwiche et al 1989; Martone et al. 2009; Espiñeira et al. 2011; Yaich et al. 2015).

Nowadays, a highly innovative phase to obtain derivative cellulose (DC), more frequently referred to as microcellulose and nanocellulose, is being developed in the consolidated cellulose industry (Ioelovich 2022). These forms of cellulose can be used as a filler in the manufacture of composites, either as a coating or in thin films, achieving very interesting and promising properties (Thomas et al. 2018). The surprising technological evolution involving DC was reported in a very recent review of patents published from 2010 to 2017, suggesting a growing trend for the following years (Charreau et al. 2020). DC production requires the disintegration of cellulose fibers into particles with micro or nanoscale diameters. This process employs various chemical methodologies, among which strong acid hydrolysis is considered one of the most effective. However, the use of large amounts of hydrochloric, hydrobromic or sulfuric acids makes this method harmful to the environment (Trache et al. 2020). More recently, the use of ionic liquids (ILs) for dissolving cellulose has grown, as they are regarded as environmentally friendly being reusable, non-corrosive, non-volatile and non-flammable (Shamsuri et al. 2022). Ionic liquids are salts composed entirely of ions that interact with the hydroxyl protons of cellulose, thus breaking its strong intermolecular hydrogen bonds. Swatloski et al. (2002) have postulated that ILs are capable of direct hydrolyzing cellulose with the application of mild heating or microwave energy. Further, imidazolium ionic liquids are most used in decomposition of cellulose and in the preparation of DC material (Singh et al. 2017).

In general, to achieve profitable valorization of seaweeds biomass, it is essential to co-produce multiple unique biochemical components with demonstrated market value. Therefore, the full potential of seaweed biomass can be realized through a sequential extraction strategy, enabling the production of multiple value-added products. *Ulva ohnoi* Hiraoka & Shimada is successfully farmed by PROMAC-Blue Evolution, a commercial cultivation system located in Baja California (Mexico) and its production is mainly marketed as human food. However, other potential applications can be explored, such as using seaweed biomass as a source of economically important polysaccharides. The main goal of this study is to valorize the cell wall polysaccharides of this biomass as potential producers of ulvan and cellulosic materials through a sequential extraction approach that utilize, as far as possible, eco-friendly reagents. For this purpose, in the extraction of cellulose the traditional bleaching agent sodium chlorite ($NaClO_2$) will be replaced by hydrogen peroxide (H_2O_2), and IL will be used to obtain DC. In addition, microwave-assisted extraction (MAE) will be also employed as environmentally friendly technology. This study examines and discusses the physicochemical, structural, and biological properties of the extracted polysaccharides.

Material and methods

Algal material

Ulva ohnoi cultivated and harvested from a commercial aquaculture system was provided by Productos Marinos de las Californias (PROMAC) and Blue Evolution located at Baja California, Mexico (Fig. 1). The material analyzed is a representative sample of the whole commercial cultivated biomass collected on January 2022 (Lot#017–22-GU80-O). After harvesting, drying and milling the whole batch 1 kg dry weight sample was taken. This was considered as the initial biomass to be analyzed, from which subsamples were taken as replicates. All the extracted polysaccharides and their chemical analysis were performed in triplicate (n = 3). C and N elemental analysis was performed in seven samples of dry tissue (n = 7).

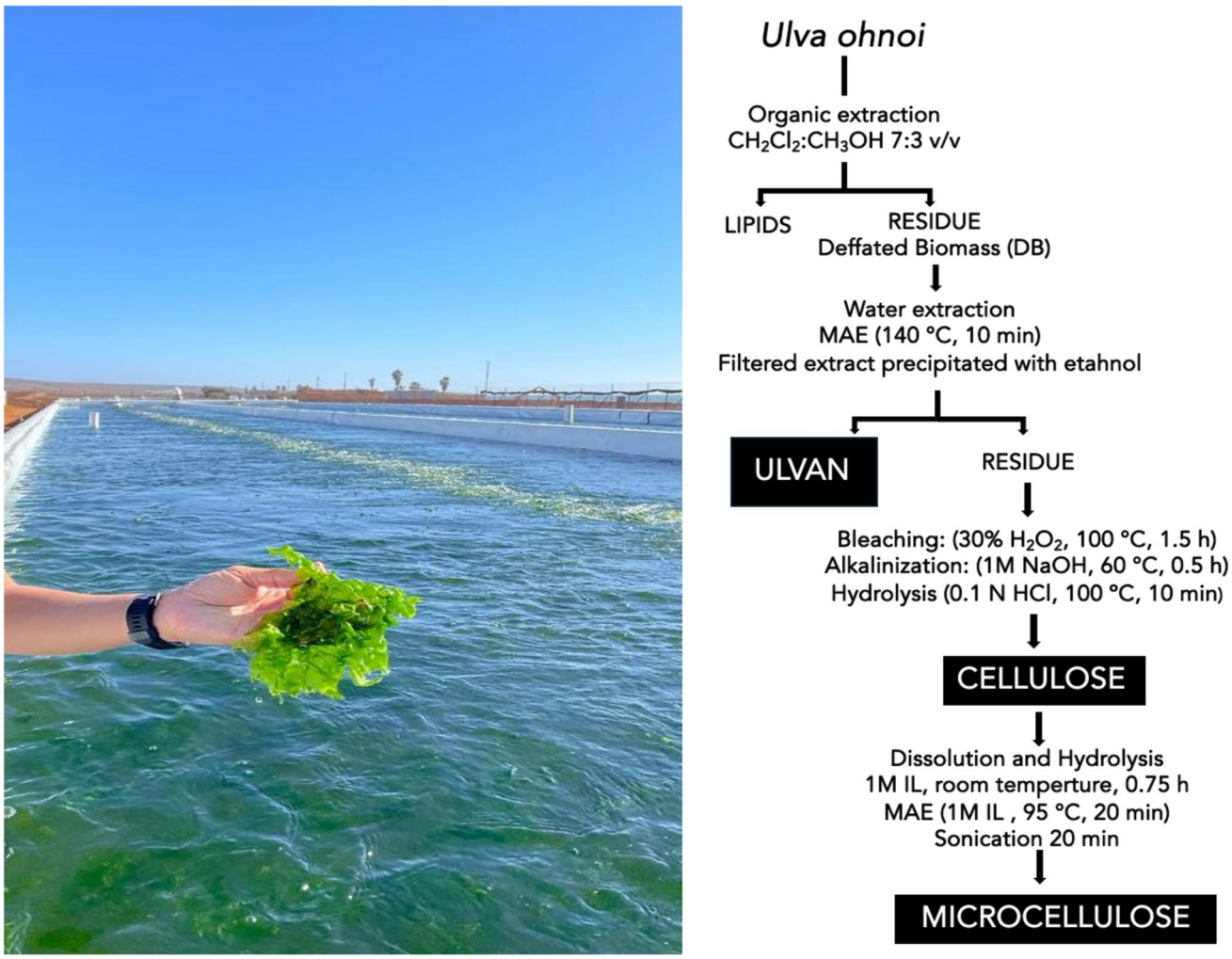


Fig. 1 Schematic representation of the sequential extraction process of *Ulva ohnoi* biomass harvested from the PROMAC-Blue Evolution cultivation facilities

Biochemical composition of the cultured Ulva ohnoi

Determination of total soluble carbohydrates was performed by the phenol sulfuric acid method (Dubois et al. 1956), whereas protein was determined by the Lowry et al. (1951) method with bovine serum albumin as protein standard. Lipid content was evaluated with 50 mL dichloromethane/methanol (7:3 v/v) following the method of Bligh and Dyer (1959).

An estimation of the lignin-like content of *U. ohnoi* was obtained employing the FiberCap System specifically designed for fiber following the Weende and van Soest method (Van Soest 1973). Briefly, an acid detergent extraction step to remove protein and other components from the cellulose was performed using 1.0 N H_2SO_4 with cetyltrimethylammonium bromide (CTAB), boiling for 1 h. For lignin determination, the produced acid detergent fiber was subsequently treated with 72% H_2SO_4 for 3 h at room temperature, to isolate the acid detergent lignin.

Sequential extraction of cell wall polysaccharides

To obtain ulvan, cellulose and derivative cellulose (DC), an integrated processes and sequential extractions was carried out using 1 g seaweed (dw) as illustrated in Fig. 1. In general, during extraction of sulfated polysaccharide like ulvan from seaweeds, interfering substances such as pigments and lipids may also be co-extracted, potentially affecting purity. Therefore, their removal is often considered an essential purification step. Thus, lipids were first extracted and discarded (Bligh and Dyer 1959), and the remaining defatted biomass (DB) was processed to extract ulvan. For comparison, ulvan from non-defatted biomass (NDB) was also processed. Ulvan was extracted by MAE according to

Freile-Pelegrín et al. (2020) using Microwave Accelerated Reaction System (MARS 800 W, CEM, USA). Briefly, dried powder sample was suspended in distilled water in a 1:50 (w/v) proportion and extracted into a closed vessel system (OMNI XP 1500). Microwave thermal history consisted of 5 min heat-up and 10 min extraction time at 140 °C. The ulvans was further isolated by ethanol precipitation, dried at 60 °C for 24 h, and weighed to calculate yield. The insoluble residue was dried and weighed.

The leftover insoluble residue recovered after ulvan extraction was used to obtain crude cellulose following the method described in Freile-Pelegrín et al. (2020). Briefly, the residual biomass from the previous steps was soaked in 30% active H_2O_2 solution at a ratio of 1:50 (w/v) and heated at 100 °C for 1.5 h for bleaching. After filtration, the bleached algal residue was treated with 1 M NaOH solution (1:50 w/v) at 60 °C for 0.5 h. The alkali-treated sample was washed with distilled water to reach pH of 7 and then, filtered. The solid algal residue was resuspended in 0.1 N HCl (1:50 w/v) for 10 min at 100 °C. The resultant slurry was cooled at room temperature, washed with water to remove excess acid, filtered, and freeze dried to obtain crude cellulose, expressed relative to the initial algal biomass. To determine the crystalline fraction of the crude cellulose, α- and β-cellulose were then obtained as described in Freile-Pelegrín et al. (2020). Briefly, dried cellulose was soaked in 17.5% NaOH (1:30 w/v) at 20 °C for 2 h. The slurry obtained was centrifuged at 5000 rpm for 15 min. The supernatant was removed by decantation, and α-cellulose (residue) was obtained after repeated water washing until pH 7. The α-cellulose was collected by freeze-drying and weighed to calculate yield relative to the crude cellulose. The β-cellulose was then precipitated from the supernatant using 20 mL of 3 N H_2SO_4, recovered by centrifugation, washed with water to remove residual acid, and weighed to calculate the yield.

For the preparation of DC, the previously obtained crude cellulose was subjected to dissolution and hydrolysis. For this purpose, a new procedure was proposed using both IL and MAE which was based on different previously reported methodologies (Ohno and Miyafuji 2013; Kos et al. 2014; Chowdhury and Hamid 2016; Singh et al. 2017; Shamsuri et al. 2022). The sample was first pretreated with 1 M IL (1-ethyl 3-methylimidazolium chloride) in a ratio of 1:20 (w/v) for 0.75 h at room temperature to promote the cellulose dissolution process. The hydrolysis reaction was then completed by MAE in a closed vessel OMNI XP, and the microwave thermal history consisted of 10 min heat-up followed by 20 min at 95 °C. The reaction was quenched by adding cold distilled water resulting in the formation of DC which is insoluble in this solvent. The derivative cellulosic material was separated from the solution by centrifugation (4500 rpm for 20 min). After removing the supernatant, the solid fraction was sonicated in an ultrasonic bath at room temperature for 20 min to reduce aggregate size. The samples were then centrifuged and washed repeatedly to remove IL residues and finally, freeze dried to obtain yield based on crude cellulose.

Chemical analysis of ulvan

Sulfate content was determined by the barium chloride-gelatin turbidimetric assay (Jackson and McCandless 1978). Uronic acids content was measured with a modification of the carbazole method (Blumenkrantz and Asboe-Hansen 1973; Filisetti-Cozzi and Carpita 1991). Total phenolic content (TPC) of ulvans was determined using the Folin-Ciocalteu reagent. Twenty microliter of 0.1 g mL^{-1} was transferred to a 96-well plate. Subsequently, 100 µL of a solution of Folin-Ciocalteu reagent (1:10), 40 µL of sodium carbonate (1 M) and 20 µL of distilled water were added. The plate was incubated at room temperature for 60 min in dark and the absorbance was recorded at 760 nm. A calibration curve was constructed using gallic acid (10–110 µg mL^{-1}) and TPC was expressed as milligram of gallic acid equivalents per 100 g (mg GAE $(100\ g)^{-1}$). Protein content of ulvans was determined according to Bradford (1976), with some modifications. Ten microliter of 0.05 g mL^{-1} of ulvan solution was placed in a well of 96-well plate and 90 µL of Bradford reagent was added. Samples were incubated at room temperature for 10 min and absorbance was measured at 595 nm. A calibration curve was constructed with bovine serum albumin (25–300 µg mL^{-1}). Content of protein was expressed as milligram of bovine serum albumin equivalent per 100 g (mg BSA $(100\ g)^{-1}$).

Fourier Transform Infrared (FTIR) analysis

To validate the ulvan and cellulose structures extracted FTIR spectra were obtained using a NICOLET IS5 FTIR spectrophotometer (Thermo Fisher Scientific, USA) using the attenuated total reflection (ATR) technique. Each spectrum was recorded with 64 scans within the spectral range of 4000–650 cm^{-1} and a resolution of 4 cm^{-1}.

X-ray Diffraction (XRD) pattern

XRD patterns of ulvan and cellulose were recorded at room temperature in a Siemens model D5000 (Germany) diffractometer with Bragg Brentano geometry and monochromatic CuKα radiation (λ = 1.5418 Å). The angle 2θ was set between 5 and 60°. The crystallinity index (CI) was calculated using the equation reported by Segal et al. (1959) and described as:

$$CI = \left(I_{max} - I_{min}\right)/I_{max}$$

where I_{max} is the intensity of the highest peak at 2θ about 22° and I_{min} is the minimum intensity at a 2θ close to 18° corresponding to the amorphous regions of the cellulose I.

Scanning electron micrograph (SEM)

Morphological changes from crude cellulose to DC were observed using a scanning electron microscope coupled with energy-dispersive spectroscopy (SEM–EDS, model Phillips XL-30 ESEM JEOL JSM-7600F, Japan) with a voltage of 10 and 15 kV, and at 50, 500 and 1500 × magnification.

Antioxidant activity of ulvans

Ulvan solutions at a concentration of 0.1 g mL^{-1} in water were prepared. Then, 300 µM DPPH (2,2-diphenyl-1picryllhydrazyl) and 40 mM TPTZ (2,4,6-Tris(2-pyridyl)-s-triazine) reagents were used to determine the ascorbic acid equivalents antioxidant capacity (AEAC) and the ferric reducing antioxidant power (FRAP) according to the methods of Chale-Dzul et al. (2017) and Henderson et al. (2015), respectively. The absorbances for DPPH and FRAP assays were measured at 517 and 593 nm, respectively. Ascorbic acid (AA) was used to construct a calibration curve for the DPPH assay (1–20 µg mL^{-1}) and the FRAP assay (6.25–200 µg mL^{-1}). Results for both assays were expressed as milligram of AA equivalents per 100 g (mg AA $(100\ g)^{-1}$). Each experiment was done in triplicate.

To evaluate ulvan toxicity a cell viability test was performed using an MTT (3-(4,5-dimethylthiazol-2-yl)−2,5-diphenyltetrazolium bromide). The human hepatoma cell line (HepG2) was growing in sterile Costar 75-cm^2 flasks containing Roswell Park Memorial Institute (RPMI) medium supplemented with fetal bovine serum (SFB) 10%, 100 U mL^{-1} penicillin, and 100 µg mL^{-1} streptomycin for 48 h at 37 °C in atmosphere of 5% CO_2 and 95% humidity. The HepG2 cell line was plated at density of 5×10^3 cells per well in a 96-well microtiter and incubated under the conditions described above. After 48 h, cells were treated with ulvan (2000–1.95 mg mL^{-1}) and incubated for 24 h. The plates were rinsed with phosphate-buffered saline, and 10 µL of MTT solution (5 mg mL^{-1}) was added. They were incubated for 4 h at 37 °C (Mosmann 1983). Finally, the medium was removed, and the formed formazan crystal were dissolved with 100 µL of acidified isopropanol (0.4 N HCl). The absorbance was measured at 540 nm. The concentration of ulvan that killed 50% of the cells (CC_{50}) was calculated using GraphPad Prism 9.0 software (USA).

Statistical analyses

Results are expressed as means ± standard deviation (n = 3). The software SPSS program (v24.0) was used for statistical analysis. One-way analysis of variance (ANOVA) was tested with the non-parametric Kruskal–Wallis test. For the antioxidant assays, Welch's t test was used to assess differences between extraction procedures (ulvans from DB *vs* NDB). The analysis was performed using GraphPad Prism 9.0 Software to establishing statistical significance; value of $p < 0.05$ were considered significant.

Results

The results of the initial proximate composition of cultivated *U. ohnoi* including moisture, ash, carbohydrates, proteins, and lipid content, and elemental C and N are summarized in Table 1. The estimations of C:N ratio (7.05) and lignin-like content (~ 8%) in the algal tissue are also shown.

Cell wall polysaccharides extracted

Ulvan and cellulose were obtained using the proposed sequential extraction process (Fig. 1) and their yields are presented in Table 1. The residual biomass from lipid extraction (~ 93.3% dw), referred to as DB, was processed to extract ulvan, yielding 22.7 ± 2.5% dw based on the initial biomass. No significant difference was observed in the ulvan yield extracted from NDB (see Table 1). In the next step of the sequential extraction process, the residual biomass from ulvan extraction (~ 77.4% dw) was processed to obtain crude cellulose (3.8 ± 0.1%). The yields of α- and β-cellulose fractions of crude cellulose, as well as the α/β-cellulose ratio (3.9) were also determined (Table 1). Furthermore, derivative cellulose (DC) was subsequently obtained from the crude cellulose using IL and MAE, achieving a yield of 95.6 ± 1.6% relative to the crude cellulose.

FTIR analysis

The polysaccharide nature of both ulvan (Fig. 2) and crude cellulose (Fig. 3), sequentially extracted from the cultured *U. ohnoi,* was confirmed by the presence of characteristic absorption bands (Robic et al. 2009). The broad and sharp signals around 3300 cm^{-1} correspond to the O–H stretching vibration resulting from intermolecular and intramolecular hydrogen bond within the polysaccharide structure, while the peaks around 2900 cm^{-1} correspond to the stretching vibrations of the methylene bonds (C–H), which are also characteristic in polysaccharides.

The FTIR spectra of ulvan from DB and from NDB were practically identical (Fig. 2), exhibiting characteristic

Table 1 Biochemical composition and polysaccharide yields of commercially cultivated *Ulva ohnoi* biomass by the sequential extraction

	Parameter	
Ulva ohnoi content	Moisture (% dw)	96.0 ± 0.13
	Ash (% dw)	25.9 ± 1.30
	Carbohydrates (% dw)	26.3 ± 0.65
	Proteins (% dw)	13.8 ± 0.51
	Total lipids (% dw)	6.7 ± 0.05
	C (% dw)	28.2 ± 0.27
	N (% dw)	4.0 ± 0.05
	C/N	7.05
	Lignin-like content (% dw)	7.97 ± 0.11
Cell wall polysaccharides	Ulvans from DB (% dw)	22.7 ± 2.5[a]
	Sulfate (% dw)	20.6 ± 0.72[a]
	Uronic acids (% dw)	21.9 ± 0.77[a]
	TPC (mg GAE (100 g)$^{-1}$)	0.019 ± 0.00[a]
	Proteins (mg BSA (100 g)$^{-1}$)	4.00 ± 0.05[a]
	Ulvans from NDB (% dw)	22.5 ± 0.51[a]
	Sulfate (% dw)	20.3 ± 0.81[a]
	Uronic acids (% dw)	22.8 ± 0.52[b]
	TPC (mg GAE (100 g)$^{-1}$)	0.015 ± 0.00[a]
	Proteins (mg BSA (100 g)$^{-1}$)	3.71 ± 0.12[a]
	Crude cellulose (% dw)	3.8 ± 0.10
	α-cellulose (% of crude cellulose)	24.8 ± 3.4
	β-cellulose (% of crude cellulose)	6.3
	Micro-cellulose (% of crude cellulose)	95.6 ± 1.6

DB Defatted biomass; *NDB* Non-defatted biomass; *TPC* Total phenolic content; *GAE* Gallic acid equivalents *BSA* Bovine serum albumin equivalents

The yields are referred to the initial material in dry weight (dw). Data presented are mean ± standard deviation. Different letters indicate significant differences ($p < 0.05$)

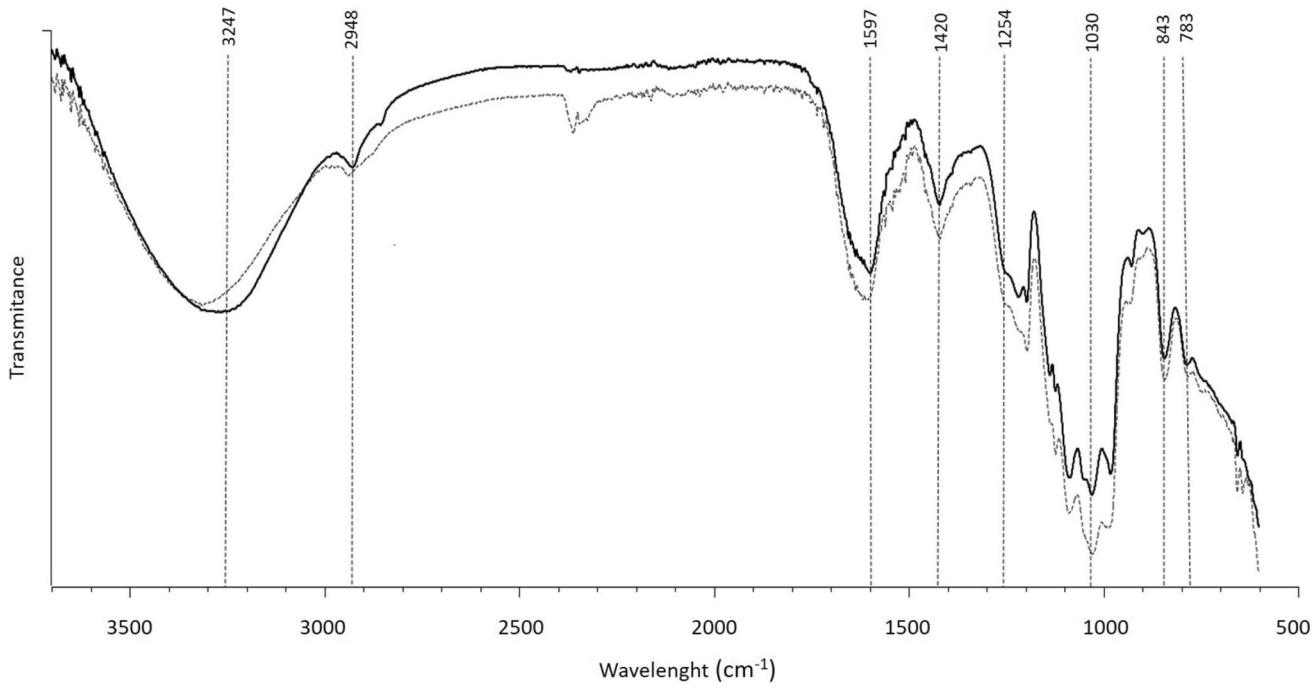


Fig. 2 FTIR spectra of ulvans extracted from defatted biomass (DB, solid line) and non-defatted biomass (NDB, dotted line) of *Ulva ohnoi*

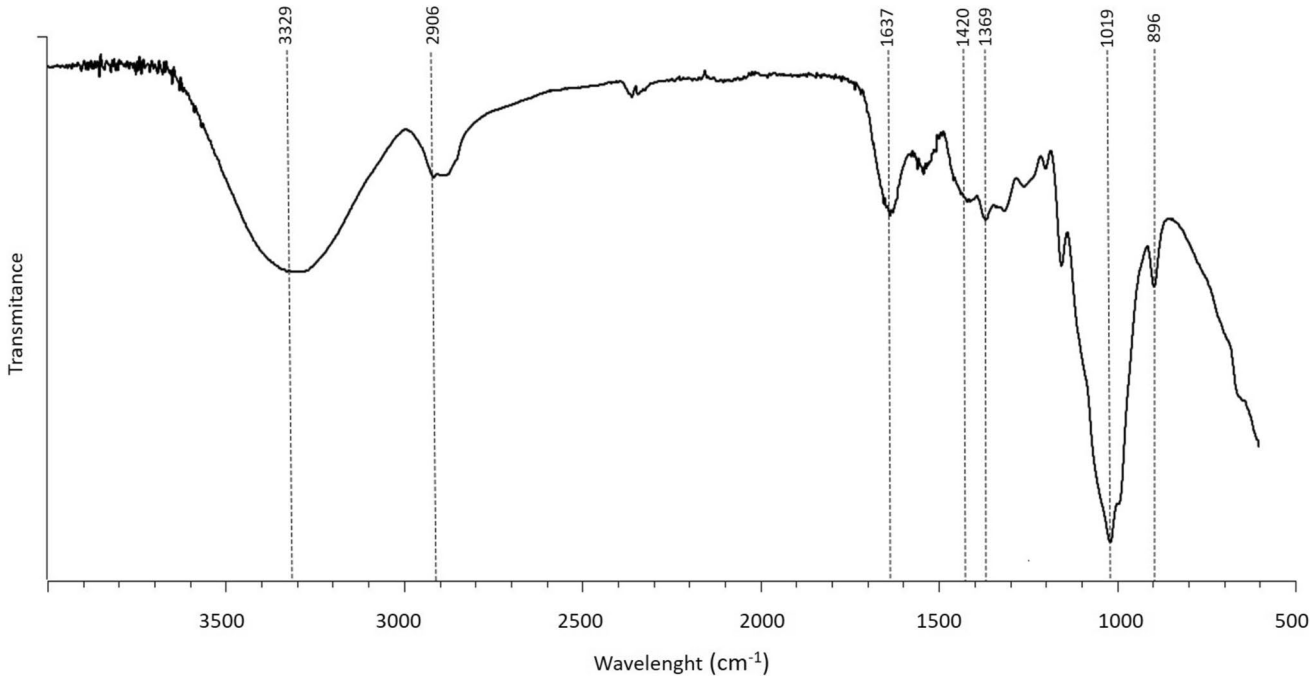


Fig. 3 FTIR spectrum of crude cellulose sequentially extracted from *Ulva ohnoi* biomass

fingerprint signals corresponding to sulfate and carboxyl groups. This is supported by chemical analysis, which showed sulfate and uronic acid contents of approximately 21% and 22%, respectively (Table 1). The peak observed at 1254 cm^{-1} is associated with S = O stretching vibration of sulfate groups (Toskas et al 2011; Thanh et al. 2016). The presence of carboxylic acids (COO-) is shown in bands at 1597 cm^{-1} and at 1420 cm^{-1} denoting the presence of uronic acids and confirming the presence of glucuronic and iduronic acid units (Chen et al. 2021). A maximum absorption band was identified at around 1030 cm^{-1} likely due to C–O-C stretching from the two main sugars, rhamnose and glucuronic acid (Robic et al. 2009). The bands at 843 and 783 cm^{-1} correspond to the vibration of the C–O–S bond of the sulfate in the axial and equatorial positions (Toskas et al. 2011) confirming the sulfated nature of the extracted ulvans. The weak signals at around 1650 cm^{-1} and 1540 cm^{-1} were indicative of the presence of proteins (Freile-Pelegrín et al. 2020), which was confirmed by the chemical analyses as is shown in Table 1. Furthermore, the chemical analyses, sulfate, protein, and TPC did not show statistically significant differences between ulvans from DB and from NDB, although a slightly higher content of uronic acids ($p < 0.05$) was found in ulvan from NDB (Table 1).

The FTIR spectrum of crude cellulose (Fig. 3) showed a typical cellulose pattern with a sharp peak at 1637 cm^{-1} corresponding to the vibrations of water molecules absorbed by cellulose. The peaks at 1420 cm^{-1} and 1369 cm^{-1} are related to the H-C-H scissor and H-C-H vibrations of α-cellulose (Wahlström et al. 2020). The C–O–C pyranose ring skeletal vibration was identified a prominent band at 1019 cm^{-1}. Ether bonds are an essential part of the cellulose backbone, linking glucose through β-1,4-glucosidic bonds. The characteristic peak at around 896 cm^{-1} is an indicator for the presence of β-glycosidic bond between glucose units in cellulose (El-Gendy et al. 2023). The absence of sulfated polysaccharide with characteristic peaks around 840 and 780 cm^{-1} would confirm an efficient extraction of ulvan in the previous step. Furthermore, the absence of shoulder peak at around 1730 cm^{-1} as well as other at around 1600 and 1406 cm^{-1} related to the vibration of the aromatic ring indicates no appreciable lignin content (Kostryukov et al. 2023).

XRD analyses

The XRD pattern of ulvans (Fig. 4) showed dispersed signals around $2\theta = 20°$ with neither sharp nor defined diffraction peaks, characteristic of amorphous structures.

The XRD pattern of both crude cellulose and its α-cellulose fraction are shown in Fig. 5. In general, the XRD displayed a diffraction profile like that expected for typical cellulose I structure found in green seaweeds, with peaks around $2\theta = 16°$, 22°, and 34° which are attributed to the (100), (200) and (004) crystalline planes of cellulose I respectively (Mihranyan 2011; Doh et al. 2020). Thus, for crude cellulose, the distinctive peak corresponding to the crystal structure was observed at $2\theta = 21.78°$, whereas

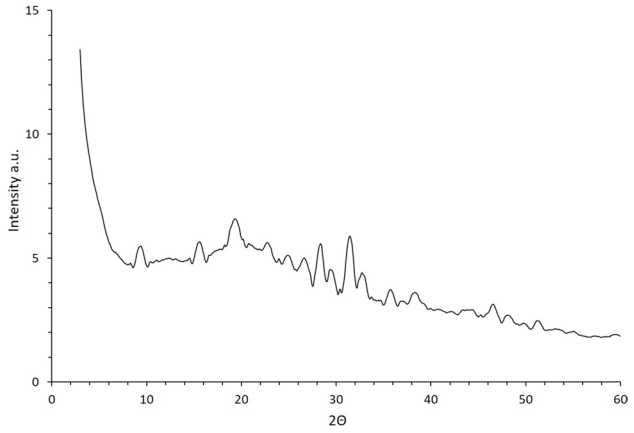


Fig. 4 XRD pattern of ulvan extracted from defatted biomass (DB) from *Ulva ohnoi*

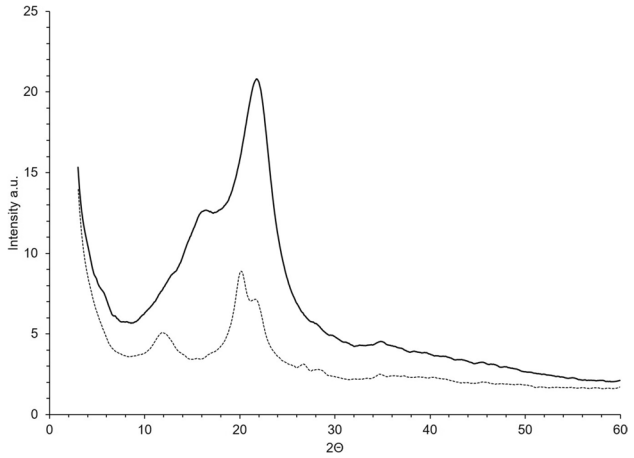


Fig. 5 XRD patterns of crude cellulose (solid line) and α-cellulose fraction (dotted line) sequentially extracted from *Ulva ohnoi* biomass

for α-cellulose, it appeared at 20.12°. The peaks related to the (004) crystalline plane were too weak, which is characteristic of amorphous fraction (Doh et al. 2020). From the above results, the crystallinity index (CI) was calculated, resulting values of 0.39 and 0.65 for crude cellulose and α-cellulose, respectively, indicating semicrystalline characteristics.

Antioxidant activity of ulvans

Regarding biological activity, ulvans extracted from both DB and from NDB exhibited antioxidant activity without cytotoxicity ($CC_{50} > 1000$ µg mL^{-1}) (Table 2). Ulvan from NDB exhibited higher antioxidant activities compared to ulvan from DB ($p < 0.05$), as measured by both DPPH (expressed as AEAC) and FRAP assays.

Table 2 Antioxidant activity and cytotoxicity of ulvans extracted from *Ulva ohnoi* biomass. Data presented are mean ± standard deviation. Different letters indicate significant differences ($p < 0.05$)

Ulvans	AEAC (mg AA (100 g)$^{-1}$)	FRAP (mg AA (100 g)$^{-1}$)	CC_{50} (µg mL^{-1})
DB	1.40 ± 0.08^{a}	0.65 ± 0.04^{a}	$> 1000^{a}$
NDB	2.73 ± 0.09^{b}	0.89 ± 0.02^{b}	$> 1000^{a}$

DB Defatted biomass; *NDB* Non-defatted biomass; *AEAC* Ascorbic acid equivalents antioxidant capacity; *AA* Ascorbic Acid; *FRAP* ferric reducing antioxidant power

SEM of crude cellulose and DC

The SEM images of crude cellulose and DC are presented in Fig. 6. Treatment with IL, MAE and ultrasonic bath drastically altered the size of crude cellulose (Fig. 6A), resulting in DC particles with thickness and length in a micrometer range of approximately 50–200 µm (Fig. 6B). These dimensions are typical of microcellulose (Ioelovich 2022). SEM images at higher magnification (500× and 1500×) revealed a smooth, flat surface for crude cellulose (Fig. 6C,E), which transformed into a fibrous, honeycomb-like structure after treatment (Fig. 6D,F).

Discussion

Ulva represents an important raw material due to its nutritional value and its high cultivation potential. Within the framework of a sustainable seaweed economy, diversification and the use of sequential extractions can enhance biomass utilization. In the present study, cultivated and marketed *Ulva ohnoi* from PROMAC-Blue Evolution was successfully utilized to obtain other valuable component from the harvested biomass such as polysaccharides.

In general, the biochemical composition of *U. ohnoi* was within the range of values previously reported for this species in culture (Glasson et al. 2017; Revilla-Loano et al. 2021; Alamrousi et al. 2022; Souza-Rocha et al. 2023; Bodar et al. 2024). However, it should be noted that carbohydrate and protein contents, as well as the C/N ratio, can vary depending on culture conditions and, consequently, the nutritional status of alga. In the present study, soluble carbohydrate and ash were the primary contributors to the total biomass, accounting for 52.2% dw, followed by protein and lipids (20.5% dw). These results confirm that this species is primarily marketed for human consumption. Specifically, *U. ohnoi* was rich in carbohydrates (26.3%), with soluble ulvans appearing as one of the main components and thus representing a potential valuable resource.

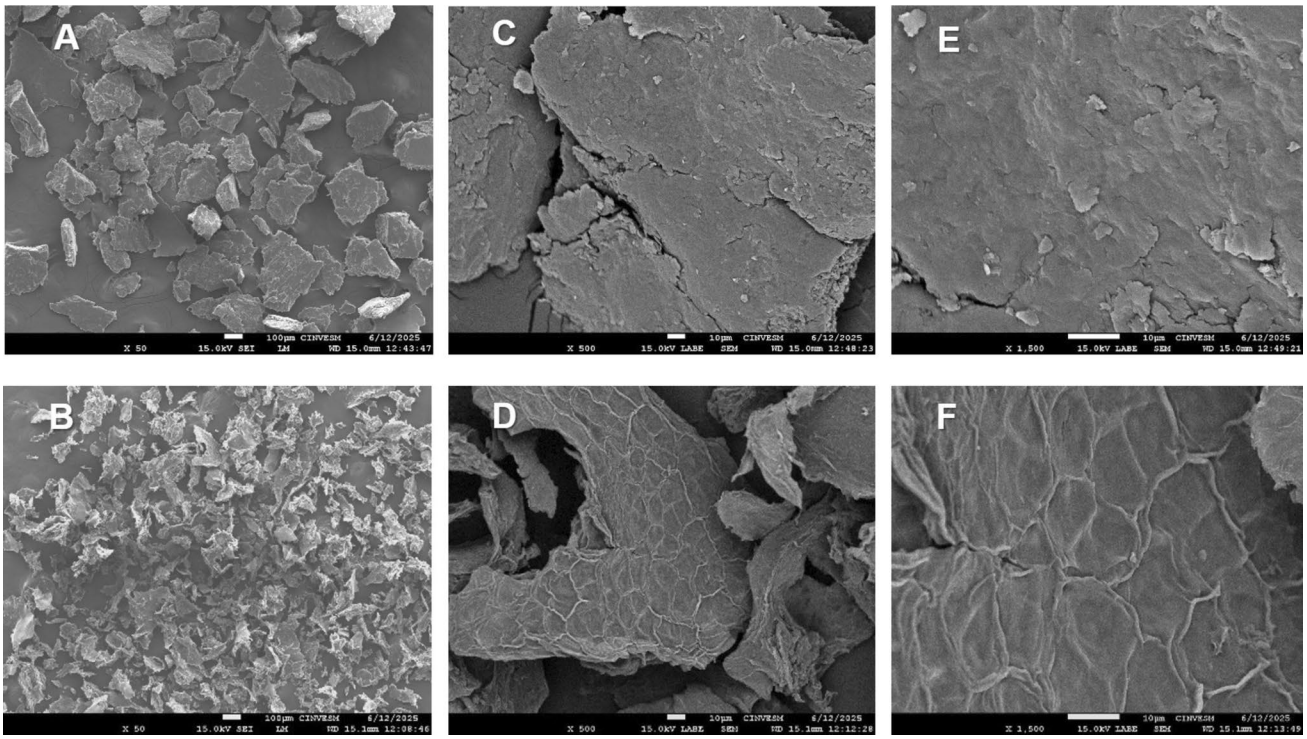


Fig. 6 SEM images of crude cellulose (**A,C,E**) and micro-cellulose (**B,D,F**) extracted from *Ulva ohnoi* biomass. The scale bars correspond to 100 µm for (A) and (B), and 10 µm for (C-F)

In the sequential extraction process, the first step involved discarding a relatively high amount of lipids (6.7% dw). To maximize the utilization of *U. ohnoi* biomass, further studies are recommended to valorize these lipids, given that *Ulva* species area known to contain elevated levels of polyunsaturated fatty acids (PUFAs), including omega-3 and omega-6 fatty acids (Moustafa and Batran 2014).

As a second step of the sequential extraction process, ulvans was obtained. Our results showed an ulvan yield of approximately 22% dw (Table 1), which is considerably higher than the yields reported by Glasson et al. (2017) and Prabhu et al. (2020) for the same species from cultivation, where values ranged from 3.7 to 13.8%, also using a cascading biorefinery approach. It is interesting to note that both yield and structure of ulvans remained consistent whether extracted from DB or NDB. The ulvan structure was confirmed by FTIR and, as expected, XRD revealed an amorphous structure similar to ulvans from other species of green seaweeds (Freile-Pelegrín et al. 2020). Structural and chemical analysis indicated that the ulvan consisted of a heteropolysaccharide with high contents of sulfates and uronic acids, comparable to that reported for other species of the order Ulvales with sulfate and uronic acid contents varying between 14–32% and 6.5–19%, respectively (Lahaye and Robic 2007; Thanh et al. 2016; Tziveleka et al. 2019). In the present study, a low protein content was obtained in the ulvans, consistent with findings for ulvan extracted from *Ulva pertusa* (Chen et al. 2021).

Regarding biological activity, both ulvans from DB and from NDB exhibited antioxidant capacity, as also shown by Prabhu et al. (2020) and Chen et al. (2021) for ulvans from *U. ohnoi* and *U. pertusa*, respectively. Comparatively, the ulvan from NDB showed greater activity in both DPPH (expressed as AEAC) and FRAP tests. It is well stablished that both sulfates and uronic acids have a significant effect on the antioxidant activity, due to a strong capacity for hydrogen donation and for metals chelation, as well as to its effectiveness as scavengers of free radicals (Qi and Sun 2015). However, ulvan is a complex carbohydrate that can additionally contain small amounts of other bioactive compounds including lipids, proteins and phenolic compounds (Kidgell et al. 2019). In the present study, ulvans extracted from DB and NDB exhibited practically the same structure and chemical composition, except for differences in lipid content and a slightly higher uronic acids content in ulvan from NDB, which may contribute to its greater antioxidant activity. However, to gain a better understanding, more detailed physicochemical and structural studies are recommended, since accurate chemical characterization including the main constituents and molecular weight is essential for interpreting the potential biological activities of the ulvans (Kidgell et al. (2019).

Following ulvan extraction, crude cellulose was obtained with a yield of 3.8%, which is lower than the 8.7% reported by Prabhu et al. (2020) for the same species. However, this value falls within the range reported for other *Ulva* species (2.2–10%) (Wahlström et al. 2020; Gomaa et al. 2022; El-Gendy et al. 2023). As a result of increasing demand for cellulose and its derivatives together with growing environmental awareness, the identification of alternative renewable raw materials seems essential. Although the cellulose yield from cultivated *U. ohnoi* was not particularly high, this species can still considered promising source of cellulose for several reasons: (1) *U. ohnoi* exhibits high productivity and can be cultivated on a large-scale using technologies that do not require freshwater, arable land, fertilizers, or pesticides (Revilla-Loano et al. 2021). (2) It contains abundant and diverse carbohydrates, including cellulose with a low lignin-like content of 7.9% which is comparable to values reported for other *Ulva* species (Yaich et al 2015; Moral et al. 2019; Kolo et al. 2024), and significantly lower than the lignin content in woody biomass (30–60% dw) and grasses (10–30% dw) (Baghel et al. 2021 and references therein). The sequential extraction process proposed in this study appears to be effective for lignin-like compound removal, as evidenced by the absence of characteristic lignin absorption bands in the FTIR (Fig. 3). This likely enhanced cellulose accessibility, enabling extraction under milder conditions and through more environmentally friendly sustainable processes.

In the present study the α-/β-cellulose ratio was 3.9, indicating that the highly crystalline α-cellulose fraction is nearly four times greater than the less crystalline β-cellulose fraction (Table 1). The α-/β-cellulose ratio was lower than that reported for other Chlorophyta but fell within the range observed for other species belonging to the order Ulvales (Siddhanta et al. 2011, 2013).

Since the CI reflects the proportion of crystalline regions, the dominant α-cellulose fraction in *U. ohnoi* exhibited a higher CI compared to crude cellulose (0.65 vs. 0.39), indicating a greater degree of crystallinity following the removal of amorphous components. The recorded CIs of *U. ohnoi* were comparable to those reported by Jmel et al. (2019) and Wahlström et al. (2020) for *U. lactuca* (CI 0.59 and 0.48) and by Lee et al. (2024) for *U. ohnoi* (CI 0.42) indicating characteristics of a semicrystalline structure. From the above result, crude cellulose of *U. ohnoi* seems less crystalline than those extracted from other green seaweeds such as *Chaetomorpha gracilis* (Freile-Pelegrín et al. 2020) and *Cladophora* sp. (Suciyati et al. 2021) which show highly crystalline structures with CIs 0.93. Crystallinity is a key factor in determining the quality of cellulose and, consequently, its potential applications. The high degree of order and close molecular packing in crystalline regions is due to the large number of hydrogen bonds. In contrast, a decrease in crystallinity, typical of semicrystalline structures, results in greater proportion of amorphous regions. This reduces the toughness of the cellulose but increases its flexibility, thereby broadening its range of possible applications, such as encapsulation and biocomposite (Jmel et al. 2019; El-Gendy et al. 2023).

In addition to crude cellulose, the green approach proposed in the present study allowed the recovery of another high value compound in the form of DC. The combination of IL, MAE, and sonication facilitated fragmentation and effective size reduction of the crude cellulose (Fig. 6A-B), indicating successful hydrolysis into micro-cellulose. From the SEM images, the surface of the crude cellulose is comparatively smooth, probably due to a higher content of amorphous components confirming its semi-crystalline structure that agrees with what recently reported for raw cellulose of *U. ohnoi* from Korea (Lee et al. 2024). In the present study, the use of MAE with IL allowed further removal of the non-crystalline domains, modifying the surface of the crude cellulose from smooth to rough in which fibers are fused into a relatively homogeneous macrostructure which is consistent with what has been described when cellulose is hydrolyzed using ILs (Swatloski et al. 2002). In general, dissolution process with IL takes place in two steps: initially, the solvent penetrates between the cellulose, inducing its swelling. The second step involves cross-linking, where electron donor–acceptor complexes are formed. Later, a DC is precipitated from the IL solution and its morphology varies depending on the precipitation liquid used. When using water, as in the present study, the DC morphology can present a rough texture that forms different structures (Swatloski et al. 2002; Yin et al. 2019). The presence of water in the IL significantly decreases the solubility of cellulose through competitive hydrogen-bonding to the cellulose microfibrils which inhibits solubilization. A cellulosic honeycomb-like architecture has been recently reported also for microcellulose obtained from the green seaweed *Cladophora* (Mardiyati et al. 2023).

It should be noted that micro-sized cellulose production market has grown significantly, rising from US$ 885 million in 2018 to more than US$1.2 billion in 2023 (Ioelovich 2022). Furthermore, the honeycomb-like structure of microcellulose is considered a useful and promising material with multiple applications, since the presence of well-organized micro-pores confers good structural stability and low density, also showing great potential in bio-interfaces, tissue engineering, and functional membranes (Uraki et al. 2011; Yin et al. 2019; Hurtuková et al. 2021; Mardiyati et al. 2023). Despite the promising results demonstrating the potential of cultivated *U. ohnoi* as a source of micro-cellulose, further studies are required to optimize the extraction process and enable its scale it up to industrial production levels.

Conclusion

The *Ulva ohnoi*, cultivated commercially by PROMAC-Blue Evolution represents a valuable raw material for human consumption. The findings of this study highlight the potential of this species for the co-production of high value polysaccharides, reinforcing its versatility potential as a sustainable resource. As a first step, ulvan demonstrating antioxidant capacity is obtained. From the residual biomass, a semi-crystalline cellulose can be recovered. Additionally, a sustainable and environmentally friendly method for isolating micro-cellulose from crude cellulose is presented. However, to further enhance the valorization of *U. ohnoi*, additional extraction steps could be incorporated to recover other valuable components such as lipids and salts. Further research is recommended to assess the feasibility and scalability of this integrated biorefinery approach. Although an economic analysis was not within the scope of this study, both an economic and Life Cycle Analysis (LCA) should be conducted to identify the most appropriate strategy for increasing the value of the cultivated biomass.

Acknowledgements The authors gratefully acknowledge the use of the LANNBIO Cinvestav-Mérida facilities, which are supported by the following grants: FOMIX-Yucatán 2008-108160, CONACYT LAB-2009-01-123913, 292692, 294643, 188345 and 204822. The technical assistance of Dr. William S. González-Gómez, Dr. Víctor Rejón Moo and MC Daniel H. Aguilar for FTIR, SEM and XRD analyses respectively is appreciated.

Authors' contributions Authors' contributions- Conceptualization, Y.F-P., D.R. and J.Z-G.; methodology, Y.F-P., C.C-Q. and J.C-D; investigation, Y.F-P. and D.R.; writing—original draft preparation, Y.F-P.; writing-review and editing, Y.F-P., D.R. and J.Z-G.; funding acquisition, D.R. and Y.F-P.

Funding The authors received financial support from Secretaria de Pesca y Acuacultura Sustentables del Gobierno del Estado de Yucatán (SEPASY). Project: Cultivo de Algas en Dzilam de Bravo SEPASY-ACU-003–2022.

Data availability Data sets generated during the current study are available from the corresponding author on reasonable request.

Declarations

Competing interests The authors declare no competing interests.

Open Access This article is licensed under a Creative Commons Attribution 4.0 International License, which permits use, sharing, adaptation, distribution and reproduction in any medium or format, as long as you give appropriate credit to the original author(s) and the source, provide a link to the Creative Commons licence, and indicate if changes were made. The images or other third party material in this article are included in the article's Creative Commons licence, unless indicated otherwise in a credit line to the material. If material is not included in the article's Creative Commons licence and your intended use is not permitted by statutory regulation or exceeds the permitted use, you will need to obtain permission directly from the copyright holder. To view a copy of this licence, visit http://creativecommons.org/licenses/by/4.0/.

References

Alamrousi A, Casais E, García-Cardesín É, Masaló I, Pintado J, Cremades J (2022) Influence of pH, N, P, N: P ratio, and dissolved inorganic carbon on *Ulva ohnoi* growth and biomass quality: potential implications in IMTA-RAS. Aquacult J 2:285–301

Baghel RS, Reddy CRK, Singh RP (2021) Seaweed-based cellulose: applications, and future perspectives. Carbohydr Polym 267:118241

Bligh EG, Dyer WJ (1959) A rapid method of total lipid extraction and purification. Can J Biochem Physiol 37:911–917

Blumenkrantz N, Asboe-Hansen G (1973) New method for quantitative determination of uronic acids. Anal Biochem 54:484–489

Bodar PA, Trivedi K, Mantri VA (2024) Changes in biochemical composition during the transition from vegetative to reproductive phases in *Ulva ohnoi*. Algal Res 82:103663

Bradford MM (1976) A rapid and sensitive method for the quantitation of microgram quantities of protein utilizing the principle of protein-dye binding. Anal Biochem 72:248–254

Chale-Dzul J, Freile-Pelegrín Y, Robledo D, Moo-Puc R (2017) Protective effect of fucoidans from tropical seaweeds against oxidative stress in HepG2 cells. J Appl Phycol 29:2229–2238

Charreau H, EmaCavallo E, Foresti ML (2020) Patents involving nanocellulose: Analysis of their evolution since 2010. Carbohydr Polym 237:116039

Chen J, Zeng W, Gan J, Li Y, Pan Y, Li J, Chen H (2021) Physicochemical properties and anti-oxidation activities of ulvans from *Ulva pertusa* Kjellm. Algal Res 55:102269

Chowdhury ZZ, Hamid SBA (2016) Preparation and characterization of nanocrystalline cellulose using ultrasonication combined with a microwave-assisted pretreatment process. BioResources 11:3397–3415

Delwiche CF, Graham LE, Thomson N (1989) Lignin-like compounds and sporopollenin in *Coleochaete*, an algal model for land plant ancestry. Science 245:399–401

Doh H, Le MH, Whiteside WS (2020) Physicochemical characteristics of cellulose nanocrystals isolated from seaweed biomass. Food Hydrocoll 102:105542

Dubois M, Guilles KA, Hamilton JK, Rebers PA, Smith F (1956) Colorimetric method for determination of sugars and related substances. Anal Chem 28:350–356

El-Gendy NS, Nassar HN, Ismail AR, Ali HR, Ali BA, Abdelsalam KM, Mubarak MA (2023) Fully integrated biorefinery process for the valorization of *Ulva fasciata* into different green and sustainable value-added products. Sustainability 15:7319

Espiñeira JM, Novo Uzal E, Gómez Ros LV, Carrión JS, Merino F, Ros Barceló A, Pomar F (2011) Distribution of lignin monomers and the evolution of lignification among lower plants. Plant Biol 13:59–68

Filisetti-Cozzi TM, Carpita NC (1991) Measurement of uronic acids without interference from neutral sugars. Anal Biochem 197:157–162

Freile-Pelegrín Y, Chávez-Quintal C, Caamal-Fuentes E, Vázquez-Delfín E (2020) Valorization of the filamentous seaweed *Chaetomorpha gracilis* (Cladophoraceae, Chlorophyta) from an IMTA system. J Appl Phycol 32:2295–2306

García-Márquez J, Moreira BR, Valverde-Guillén P, Latorre-Redoli S, Caneda-Santiago CT, Acién G, Martínez-Manzanares

E, Marí-Beffa M, Abdala-Díaz RT (2023) In vitro and in vivo effects of ulvan polysaccharides from *Ulva rigida*. Pharmaceuticals 16:660

Glasson CRK, Sims IM, Carnachan SM, de Nys R (2017) A cascading biorefinery process targeting sulfated polysaccharides (ulvan) from *Ulva ohnoi*. Algal Res 27:383–391

Gomaa M, Al-Badaani AA, Hifney AF, Adam MS (2022) Utilization of cellulose and ulvan from the green seaweed *Ulva lactuca* in the development of composite edible films with natural antioxidant properties. J Appl Phycol 34:2615–2626

Harsha Mohan E, Madhusudan S, Baskaran R (2023) The sea lettuce *Ulva* sensu lato: future food with health-promoting bioactives. Algal Res 71:103069

Heinze T, El Seoud OA, Koschella A (2018) Production and characteristics of cellulose from different sources. In: Cellulose Derivatives. Springer, Cham, pp 1–38

Henderson T, Nigam PS, Owusu-Apenten RK (2015) A universally calibrated microplate ferric reducing antioxidant power (FRAP) assay for foods and applications to Manuka honey. Food Chem 174:119–123

Hurtuková K, Fajstavrová K, Rimpelová S, Vokatá B, Fajstavr D, Kasálková NS, Siegel J, Švorcík V, Slepicka P (2021) Antibacterial properties of a honeycomb-like pattern with cellulose acetate and silver nanoparticles. Materials 14:4051

Ioelovich MJ (2022) Microcellulose vs nanocellulose – A review. World J Adv Eng Technol Sci 5:37

Jackson SG, McCandless EL (1978) Simple, rapid, turbidometric determination of inorganic sulfate and/or protein. Anal Biochem 90:802–808

Jmel MA, Anders N, Messaoud GB, Marzouki MN, Spiess A, Smaali I (2019) The stranded macroalga *Ulva lactuca* as a new alternative source of cellulose: extraction, physicochemical and rheological characterization. J Clean Prod 234:1421–1427

Lahaye M, Robic A (2007) Structure and functional properties of ulvan, a polysaccharide from green seaweeds. Biomacromol 8:1765–1774

Lee EH, Kim DG, Hong SJ, Kim JT, Shin GH (2024) Cellulose extraction from green algae, *Ulva ohnoi*, and its application to PVA-based antibacterial composite films incorporated with zinc oxide nanoparticles. Packag Technol Sci 37:473–485

Lowry OH, Rosebrough NJ, Farr LF, Randall RJ (1951) Protein measurement with the folin phenol reagent. J Biol Chem 193:265–275

Kidgell JT, Magnusson M, de Nys R, Glasson CR (2019) Ulvan: A systematic review of extraction, composition and function. Algal Res 39:101422

Kolo SMD, Obenu NM, Bria PM, Abi H, Seran BB, Wahyuningrum (2024) The optimization of initial treatment of seaweed *Ulva reticulata* using CEM synthesizer method for bioethanol production. J Turkish Chem Soc A 11:403–412

Kos T, Anžlovar A, Kunaver M, Huskić ŽE (2014) Fast preparation of nanocrystalline cellulose by microwave-assisted hydrolysis. Cellulose 21:2579–2585

Kostryukov SG, Matyakubov HB, Masterova YY, Kozlov AS, Pryanichnikova MK, Pynenkov AA, Khluchina NA (2023) Determination of lignin, cellulose, and hemicellulose in plant materials by FTIR spectroscopy. J Anal Chem 78:718–772

Małachowska E, Dubowik M, Lipkiewicz A, Przybysz K, Przybysz P (2020) Analysis of cellulose pulp characteristics and processing parameters for efficient paper production. Sustainability 12:7219

Mardiyati Y, Fauza AN, Steven S, Rachman OA, Dirgantara T, Hariyanto A (2023) High-performance *Cladophora*-algae-based paper for honeycomb core in sandwich-structured composite: preparation and characterizations. Polymers 15:1359

Martone PT, Estevez JM, Lu F, Ruel K, Denny MW, Somerville C, Ralph J (2009) Discovery of lignin in seaweed reveals convergent evolution of cell-wall architecture. Curr Biol 19:169–175

Mihranyan A (2011) Cellulose from Cladophorales green algae: from environmental problem to high-tech composite materials. J Appl Polym Sci 119:2449–2460

Mosmann T (1983) Rapid colorimetric assay for cellular growth and survival: application to proliferation and cytotoxicity assays. J Immunol Methods 65:55–63

Moon RJ, Martini A, Nairn J, Simonsen J, Youngblood J (2011) Cellulose nanomaterials review: structure, properties and nanocomposites. Chem Soc Rev 40:3941–3994

Moral A, Aguado R, Castelló R, Tijero A, Ballesteros M (2019) Potential use of green alga *Ulva* sp. for papermaking. Bioresources 14:6851–6862

Moustafa Y, Batran A (2014) Lipid chemistry of green macroalgae *Ulva* sp.: a potential resource for biotechnological applications in the Southern Mediterranean Sea Coast, Alexandria Shore, Egypt. Egypt J Aquat Biol Fish 18:9–20

Nagrale P (2023) Global cellulose fiber market research report-market forecast to 2030, 140 p. https://www.marketresearchfuture.com/reports/cellulose-fiber-market-2903

Ohno E, Miyafuji H (2013) Reaction behavior of cellulose in an ionic liquid, 1-ethyl-3-methylimidazolium chloride. J Wood Sci 59:221–228

Prabhu MS, Israel A, Palatnik RR, Zilberman D, Golberg A (2020) Integrated biorefinery process for sustainable fractionation of *Ulva ohnoi* (Chlorophyta): process optimization and revenue analysis. J Appl Phycol 32:2271–2282

Qi H, Sun Y (2015) Antioxidant activity of high sulfate content derivative of ulvan in hyperlipidemic rats. Int J Biol Macromol 76:326–329

Revilla-Loano S, Sandoval-Gil JM, Zertuche-González JA, Belando-Torres MD, Bernardeau-Esteller J, Rangel-KarinaLK F-A, Guzmán-Calderón JM, Camacho-Ibar VF, Muñiz-Salazar R, Ávila-López MC (2021) Physiological responses and productivity of the seaweed *Ulva ohnoi* (Chlorophyta) under changing cultivation conditions in pilot large land-based. Algal Res 56:102316

Robic AD, Bertrand JF, Sassi Y, Lerat M, Lahaye M (2009) Determination of the chemical composition of ulvan, a cell wall polysaccharide from *Ulva* spp. (Ulvales, Chlorophyta) by FT-IR and chemometrics. J Appl Phycol 21:451–456

Segal L, Creely JJ, Martin AE Jr, Conrad CM (1959) An empirical method for estimating the degree of crystallinity of native cellulose using X-ray diffractometer. Textile Res J 29:786–794

Shamsuri AA, Md. Jamil SNA, Abdan K (2022) Nanocellulose extraction using ionic liquids: syntheses, processes, and properties. Front Mater 9:919918

Siddhanta AK, Prasad K, Meena R, Prasad G, Mehta GK, Chhatbar MU, Oza MD, Kumar S, Sanandiya ND (2009) Profiling of cellulose content in Indian seaweed species. Biores Technol 100:6669–6673

Siddhanta AK, Mahesh U, Chhatbar MU, Mehta GK, Sanandiya ND, Kumar S, Oza MD, Prasad K, Meena R (2011) The cellulose content in Indian seaweed species. J Appl Phycol 23:919–923

Siddhanta AK, Kumar S, Mehta GK, Chhatbar MU, Oza MD, Sanandiya ND, Chejara DR, Godiya CB, Kondaveeti S (2013) Cellulose contents of some abundant Indian seaweed species. Nat Prod Commun 8:497–500

Singh S, Gaikwad KK, Park S, Lee YS (2017) Microwave-assisted step reduced extraction of seaweed (*Gelidiella acerosa*) cellulose nanocrystals. Int J Biol Macromol 99:506–510

Souza-Rocha J, Santos D, Martins MA, Bauer CM, Maraschin M, Hayashi L, Vieira FN (2023) Sea lettuce (*Ulva ohnoi*) cultivation in biofloc technology: growth performance and characterization of bioactive compounds. Bol Inst Pesca 49:e848

Suciyati SW, Manurung P, Sembiring S, Situmeang R (2021) Comparative study of *Cladophora* sp. cellulose by using FTIR and XRD. J Phys Conf Ser 1751:012075

Swatloski RP, Spear SK, Holbrey JD, Rogers RD (2002) Dissolution of cellulose with ionic liquids. J Am Chem Soc 124:4974–4975

Thanh TTT, Quach TMT, Nguyen TN, Vu Luong D, Bui ML, Van Tran TT (2016) Structure and cytotoxic activity of ulvan extracted from green seaweed *Ulva lactuca*. Int J Biol Macromol 93(Part A):695–702

Thomas B, Raj MC, Athira KB, Rubiyah MH, Joy J, Moores A, Drisko GL, Sánchez C (2018) Nanocellulose, a versatile green platform: from biosources to materials and their applications. Chem Rev 118:11575–11625

Toskas G, Hund RD, Laourine E, Cherif C, Smyrniotopoulos V, Roussis V (2011) Nanofibers based on polysaccharides from the green seaweed *Ulva rigida*. Carbohydr Polym 84:1093–1102

Trache D, Tarchoun AF, Derradji M, Hamidon TS, Masruchin N, Brosse N, Hussin MH (2020) Nanocellulose: from fundamentals to advanced applications. Front Chem 8:392

Tziveleka LA, Ioannou E, Roussis V (2019) Ulvan, a bioactive marine sulphated polysaccharide as a key constituent of hybrid biomaterials: a review. Carbohydr Polym 218:355–370

Uraki Y, Tamai Y, Hirai T, Koda K, Yabu H, Shimomura M (2011) Fabrication of honeycomb-patterned cellulose material that mimics wood cell wall formation processes. Mater Sci Eng C 31:1201–1208

Van Soest PJ (1973) Collaborative study of acid-detergent fiber and lignin. J AOAC Int 56:781–784

Wahlström N, Edlund U, Pavia H, Toth G, Jaworski A, Pell AJ, Choong FX, Shirani H, Nilsson KPR, Richter-Dahlfors A (2020) Cellulose from the green macroalgae *Ulva lactuca*: isolation, characterization, optotracing, and production of cellulose nanofibrils. Cellulose 27:3707–3725

Yaich H, Garna H, Bchir B, Besbes S, Paquot M, Richel A, Blecker C, Attia H (2015) Chemical composition and functional properties of dietary fibre extracted by Englyst and Prosky methods from the alga *Ulva lactuca* collected in Tunisia. Algal Res 9:65–73

Yin H, Zhan F, Yu Y, Li Z, Feng Y, Billon L (2019) Direct formation of hydrophilic honeycomb film by self-assembly in breath figure templating of hydrophobic polylacticacid/ionic surfactant complexes. Soft Matter 15:5052

Zertuche-González J, Sandoval-Gil JM, Rangel-Mendoza LK, Gálvez-Palazuelos AI, Guzmán-Calderón JM, Yarish C (2021) Seasonal and interannual production of sea lettuce (*Ulva* sp.) in outdoor cultures based on commercial size ponds. J World Aquac Soc 52:1047–1058

Zhao L, Sun Z-F, Zhang C-C, Nan J, Ren N-Q, Lee D-J, Chen C (2022) Advances in pretreatment of lignocellulosic biomass for bioenergy production: challenges and perspectives. Bioresour Technol 343:126123

Publisher's Note Springer Nature remains neutral with regard to jurisdictional claims in published maps and institutional affiliations.